Biochimica et Biophysica Acta, 602 (1980) 331—354

BBA 78963

ION MOVEMENTS IN GRAMICIDIN PORES

AN EXAMPLE OF SINGLE-FILE TRANSPORT

B.W. URBAN, S.B. HLADKY * and D.A. HAYDON

The Physiological Laboratory, University of Cambridge, Downing Street, Cambridge CB2 3EG (U.K.)

(Received April 28th, 1980)

Key words: Gramicidin pore; Single-file transport; Ion permeability

Summary

Experimental results on ion movement through gramicidin membrane channels are presented and discussed in terms of ion transport in the simplest single-file pore (for review see Urban, B.W. and Hladky, S.B. (1979) Biochim. Biophys. Acta 554, 410—429). Single-channel conductance and bi-ionic potential data for Na^+, K^+, Cs^+, NH_4^+ and Tl^+ are used to assign values to the rate constants of the model. Not all of the rate constants can be determined uniquely and simplifications are introduced to reduce the number of free parameters. The simplified model gives good quantitative fits to the experimental results for Na^+, K^+, Cs^+ and NH_4^+. For Tl^+, although the model accounts qualitatively for the salient features of the results, the quantitative agreement is less satisfactory. Predictions calculated from the model and the fitted rate constants are compared with independent data from blocking and tracer-flux measurements. In agreement with experiment, the model shows that only Tl^+ blocks the Na^+ conductance significantly. Furthermore, the exponent, n, in the tracer flux ratio rises, as observed, well above unity. The values for the rate constants suggest internal consistency of the model in that entry is always slower to singly occupied pores than to empty pores while exit is always faster from doubly as compared to singly occupied pores. The agreement between model prediction and experimental results suggests that the main features of ion transport in the gramicidin channel arise from cation-cation interaction in a single-file pore.

* Present address: Department of Pharmacology, University of Cambridge, Hills Road, Cambridge CB2 2QD, U.K.

Introduction

The analysis of experimental data for ion movements through the gramicidin pore which is presented here shows that the data are consistent with predictions from the simplest model for single-file pores [1].

At present, it is not possible to calculate from first principles the rate constants for ion movements from any proposed structure of the pore. However, we may attempt to determine their values by fitting them to experimental data. As a consequence, it is more difficult to obtain evidence that the model is correct rather than merely consistent with the data. Under these circumstances complex models seem of little use. The emphasis must lie on finding the simplest model that is consistent with the main experimental results, hoping that then we may at least understand the basic physical principles governing the system we observe.

Gramicidin A produces pores in thin lipid membranes which are permeable to monovalent cations of less than about 2 Å unhydrated radius but impermeable to divalent cations, anions and larger cations [2—10]. From these observations it is probable that the channel is too small to allow ions to pass each other at all readily. Further evidence is derived from the proposed structure for gramicidin A [11—13] and ionic tracer-flux experiments [14,15]. In the simplest model with this single-file constraint, the channel is divided into two compartments. Movement of an ion through the pore occurs by an ion entering the nearer compartment, transferring from one to the other and then leaving on the far side of the membrane.

Even this simple view of the transport process leads to an expression for the flux in terms of so many adjustable parameters that they cannot be determined from measurements of single-channel conductances in single salts and bi-ionic potentials. We have thus investigated which possible simplifying assumptions are consistent with our data. Even in its most general form, the model will not predict salient features of the data unless at least K^+, Cs^+, NH_4^+ and Tl^+ can enter pores which are already occupied. With the simplifying assumptions used in the numerical analysis, the model requires this result for Na^+ as well. Assumptions will be discussed which allow the calculation of rate constants that predict the complex behaviour of the transport process.

The conclusions based on these results have been discussed in preliminary reports, one using a simplified version of the arguments presented here [16], the other a more qualitative, informal approach [17].

Materials and Methods

Materials and experimental methods

Salts were of AnalaR grade, except for thallium salts which were obtained from BDH (Poole), $TlO \cdot COCH_3$ (96%), $TlNO_3$ (98%); Koch-Light, Ltd. (Colnbrook), TlCl (99.998%). NaCl, KCl and CsCl were roasted at 500°C. Other electrolyte solutions when exceeding 0.5 M concentration were treated by adding charcoal (Kodak, Nuchar-C-190-N) shaking the solution and then removing the charcoal by filtration. Water was distilled twice, the second time from a Pyrex still, and collected in Pyrex bottles (pH 5.6). Glyceryl monooel-

ate (Nu-Chek Prep, Elysian, MN) was dissolved in *n*-alkanes at 8 mM concentration. The alkanes (Koch-Light, Ltd., puriss grade) were passed through columns containing chromatographic alumina.

Gramicidin was added to the aqueous or lipid phases from stock solutions in ethanol. The samples used were initially [3] a pure sample of gramicidin A (kindly provided by E. Gross, NIH, Bethesda) and later, commercial gramicidin (Koch-Light, Ltd.) containing a mixture of gramicidin A, B and C (72% : 9% : 19% [18]).

Whenever possible Ag-AgCl electrodes were used with electrode asymmetries below 0.2 mV. For some of the single-channel experiments involving anions other than Cl^-, either Cl^- was added to the electrolyte in minute concentration or commercial calomel electrodes with salt bridges (Pye, Ltd., Cambridge, Catalogue No. 11161) were employed. For zero-current measurements, microelectrodes were used to minimize leakage from the salt bridges. The electrodes were pulled blunt (tip resistance approx. 1 MΩ) from borosilicate glass capillaries (Clark Electromedical Instruments, Pangbourne, Type GC120F) and filled with a saturated salt solution containing principally the anion of the test solution and some Cl^-. A chloridized silver wire was inserted and the top end of the electrode sealed off with wax. No appreciable leak could then be detected. Electrode asymmetries were typically below 1 mV and drifted by less than 1 mV during an experiment.

The black-film apparatus has been described by Fettiplace et al. [19]. The horizontal-cell type [10] with the same solution above and below the membrane was used for single-channel measurements. The current at constant applied potential was usually recorded with a Servoscribe pen recorder (Smith's Industries, London). The response time of the pen recorder was about 200 ms for 1/10th scale deflection which, in practical terms, means that channels with a lifetime of about 400 ms and longer could be resolved accurately. Hladky and Haydon [20] found that the gramicidin channel lifetimes were exponentially distributed with a mean lifetime of approx. 2 s in glyceryl monooleate/hexadecane membranes. A resolution of 400 ms means that for 18% of the channels it is not possible to measure accurate amplitudes and durations. At least 100 channels were recorded for each potential, the sign of the potential being reversed for about half of them. Several membranes were formed to obtain a better average. Channel heights were read off the chart record individually.

For zero-current experiments, the vertical-cell type was preferred [6]. The contents of the outer perspex cell could be stirred and exchanged. For an exchange, new solution was inserted at the bottom of the cell through a Pasteur pipette fed by gravity from a reservoir. Simultaneously, old solution was removed from the surface at the opposite corner via a stainless-steel needle. Using a dye, it was established that after exchanging 600 ml of solution more than 99% of the contents of the outer cell was new solution. Usually 1 l of the denser solution was run in. After about 500 ml, the exchange was interrupted to take a reading of the membrane potential. Normally, this reading did not differ from the final reading. A perspex bar divided the surfaces between the Teflon pot and the steel needle of the solution outflow which prevented the surface near the Teflon pot from being depleted of lipid and stopped the spreading of surface vibrations created while solution was withdrawn.

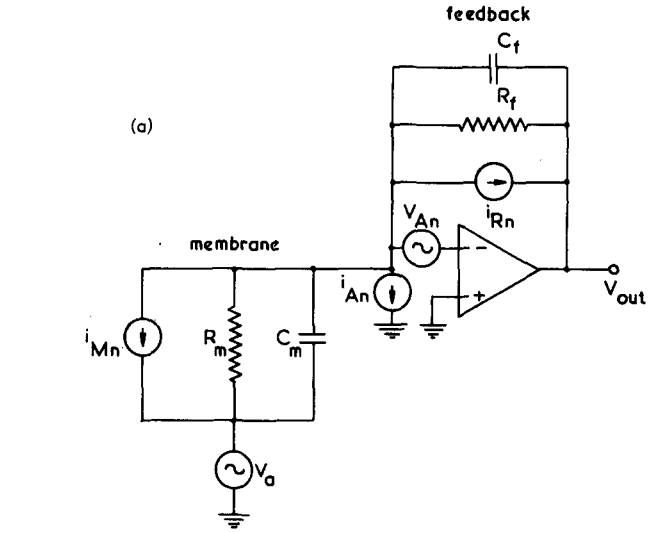

$$V_{out} = -V_a \frac{Z_f}{Z_m} + V_{Rn} \frac{Z_f}{R_f} + V_{Mn} \frac{Z_f}{R_m} + V_{An}\left(\frac{Z_f}{Z_m} + 1\right) + Z_f i_{An}$$

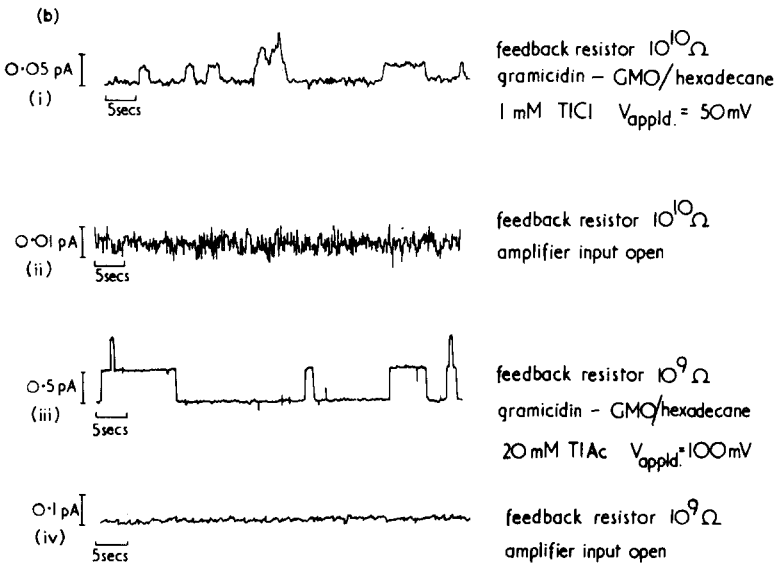

Fig. 1. (a) An equivalent circuit for the black film and the current-to-voltage amplifier including sources of noise originating from the membrane ($V_{Mn} = i_{Mn}R_m$), the feedback resistor ($V_{Rn} = \sqrt{4kTR_f\Delta f}$, where kT is the thermal energy and Δf the bandwidth), and the Analog Devices 42K operational amplifier ($V_{An} \simeq 8\ \mu V$, $i_{An} \simeq 5$ fA). The formula for the voltage at the output of the amplifier has been included. The impedances, Z_f and Z_m, are the parallel combinations of the respective feedback and membrane components. (b) Comparison of gramicidin single-channel signals with noise recorded for an open amplifier input having identical feedback characteristics. Note that the noise traces have been magnified by a factor of 5 with respect to the single-channel records. GMO, glyceryl monooleate; TlAc, $TlO \cdot COCH_3$.

For zero current, with two permeant ions present, there are still fluxes of each across the membrane and the adjacent unstirred layers. Thus, if the membrane conductance is high, the concentrations at the membrane will deviate significantly from their bulk values. Therefore, whenever a reading of the membrane potential was taken, the membrane conductance was measured as well and it was ensured that the quotient of specific membrane conductance and electrolyte concentration did not exceed 10^1 S · cm · mol^{-1}.

Particularly at low electrolyte concentration (1 mM and below), and whenever there was a considerable concentration gradient across the membrane, the zero-current potential was sometimes found to fluctuate slightly.

To determine the final microelectrode asymmetry, the microelectrodes were interchanged without breaking the membrane, this reading subtracted from the previous one and the result divided by 2.

The microelectrodes gave the membrane potential directly, except when there was a considerable concentration gradient across the membrane producing a significant difference in the electrode-tip potentials. For experiments with Ag-AgCl electrodes, the reported membrane potentials have been calculated from the measured potentials by subtracting the appropriate Nernst potentials.

Electrical apparatus and noise considerations

The electrical circuitry was the same for both types of black-film cell. One electrode was connected to a low-impedance potentiometer, the other to the negative input of a high-impedance operational amplifier (Analog Devices, 42K) used with current feedback. The electrode connections could be switched to a Vibron electrometer.

At 10 mM and less electrolyte solution, the single-channel signals become significantly affected by noise. The circuit in Fig. 1 includes different sources of noise originating from the feedback resistor, the operational amplifier, and the membrane. The resistor noise has been assumed to be solely Johnson noise; the amplifier-input noise voltage and input bias current were taken from the specification sheet for the operational amplifier 42K from Analog Devices. If there is no correlation between the various noise sources themselves and the applied potential it follows that:

$$|V|^2 = \left|V_a \frac{Z_f}{Z_m}\right|^2 + V_{Rn}^2 \left|\frac{Z_f}{R_f}\right|^2 + \left|V_{Mn} \frac{Z_f}{R_m}\right|^2 + V_{An}^2 \left|\frac{Z_f}{Z_m} + 1\right|^2 + i_{An}^2 |Z_f|^2 \qquad (1)$$

For applied potentials of 50—200 mV, a bandwidth of 1—10 Hz, values of $R = 10^9$ and 10^{10} Ω and $C = 2$ pF for the feedback circuit, it clearly follows that the amplifier voltage and current noise will be negligible. Apart from the membrane, the feedback resistor emerges as the major noise source. For a bandwidth of 1 Hz and a feedback resistor of 10^9 (10^{10}) Ω, the Johnson noise amounts to 26 μV (83 μV) corresponding to a current at the input of 0.026 pA (0.0083 pA). If the bandwidth is 10 Hz all these quantities have to be multiplied by $\sqrt{10}$. The traces ii and iv have been recorded from the operational amplifier output with only the feedback circuit connected to the negative input and are roughly in agreement with the estimate for the Johnson noise. The traces i and iii have been recorded during two single-channel experi-

ments with gramicidin at different electrolyte concentrations and should be compared with the respective noise traces from the amplifier in the test configuration for the same feedback resistance.

Numerical analysis

To calculate values for the model parameters from the existing data, the following sum of squares was minimized:

$$f(PP_x, PP_y, PP_z \ldots) = \sum_{x,a,V} \frac{[I_{th}(a, V, PP_x) - I_{exp}(a, V)]^2}{\sigma_x(a, V)^2}$$

$$+ \sum_{x,y,a} \frac{[I_{th}(a, V_{bi}, PP_x, PP_y)/W_{xy}]^2}{(a'_x + a''_y)^2} \qquad (2)$$

where PP_x symbolizes the set of parameters comprising the rate constants and the voltage parameters for the salt x, activities are denoted by the letter a, and the applied potential by V; x and y indicate the ion species involved; I_{th} is given by the flux formula (see Appendices 1 and 2); I_{exp} are experimental points; V_{bi} are the measured bi-ionic potentials; σ_x represents the estimated standard deviation of the respective conductance data point. The summation extends over all the ion species involved, and all activities and voltages where conductances and bi-ionic potentials have been measured. W_{xy} is a weight factor.

The functional form of the contribution of the bi-ionic potential experiments to the sum of squares resembles closely that of the single-channel conductances. I_{exp} at the bi-ionic potential is zero. σ_x has been replaced by activities, thus weighting roughly equally each bi-ionic data point. The weight factor allows the same importance to be assigned to the two types of data.

The numerical minimizing routine used was the NAG (Numerical Algorithm Group [21]) library routine EO4FBF. It employes the Marquardt algorithm (e.g., Ref. 22) which consists of a mixture of gradient search and approximation of the fitting function by linearization. The numerical routine requires as input data a guess for the model parameters, the data points themselves, and their respective weights which vary inversely with their estimated errors. The single-channel currents were calculated using the flux formula, but the bi-ionic potentials had to be determined iteratively as no simple analytical expression could be found. The input guess had to be reasonably close to the final answer as otherwise the procedure could converge to another local minimum. (If the flux formula is a linear function of the parameters then the sum of squares can have as many local minima as there are variables.) Local-minima traps and slow-convergence regions severely restricted any effort to search comprehensively the parameter space for minima.

A quantity called reduced χ^2 (Ref. 22, p. 84), which is basically the function, $f(PP \ldots)$, divided by the number of free data points (i.e., data points minus number of parameters), helped to judge the quality of each fit. Roughly speaking, this quantity compares the experimental error to the deviation of the theoretical prediction from the experimental data points. For a realistic estimate of the errors of the data points, χ^2 should tend to unity. The fits obtained are sensitive to an unfortunate degree to these error estimates. Accu-

rate assignment is difficult as there are many error sources present, such as statistical fluctuations of channel amplitudes, the use of a mixture of gramicidins A, B and C, noise superimposed on channels, temperature drifts (3—4% per degree Celsius), electrode potentials and unstirred-layer effects. Either underestimates or overestimates of errors can lead to a convergence away from the correct solution.

Results

Experimental data

NaCl, KCl, CsCl and NH_4Cl will be treated together as they have similar chemical properties and a common anion. Thallium salts are considered separately. TlCl is soluble only up to a concentration of 13 mM and more soluble thallium salts like $TlNO_3$ and $TlO \cdot COCH_3$ had to be used.

Transference numbers

By determining transference numbers, Myers and Haydon [6] have shown that the anion permeability of lipid membranes in the presence of gramicidin is negligible compared to that for the alkali metal ions. For thallium salts a similar result is obtained, as shown in Table I (see also Ref. 16). The anion transference number has been calculated according to Ref. 23:

$$t^- = \frac{1}{2}\left(1 + \frac{eV}{kT \ln(a''/a')}\right) \tag{3}$$

where V is the potential difference across the membrane, e the electronic charge, k the Boltzmann constant, T the absolute temperature and a the activities of the salt solutions. Although the anions are impermeable, the measured single channel currents for Tl^+ [24], K^+ [24] and Cs^+ [3] do vary a little with the species of anion present.

Single-channel conductances

In single-channel experiments, the two aqueous compartments of the bilayer chamber were filled with identical electrolyte solution, a voltage applied across the membrane, and the resulting discrete current steps (typically 0.1 to 10 pA)

TABLE I

ANION TRANSFERENCE NUMBERS IN THE PRESENCE OF Tl^+

E is the membrane potential, t^- the anion transfer number, 0.1 mM of the anion is Cl^-. Readings were taken simultaneously with microelectrodes (micro) and Ag-AgCl electrodes.

Experimental conditions	E (mV)	t^-
1.09 mM $TlO \cdot COCH_3$, 10 mM $TlO \cdot COCH_3$	52.2 (micro)	0.01
	50.7 (Ag-AgCl)	0.03
1 mM $TlO \cdot COCH_3$, 100 mM $TlO \cdot COCH_3$	99.5 (micro)	0.04
	104.9 (Ag-AgCl)	0.02
10 mM $TlNO_3$, 297 mM $TlNO_3$	68.5 (micro)	0.04
	69.8 (Ag-AgCl)	0.03

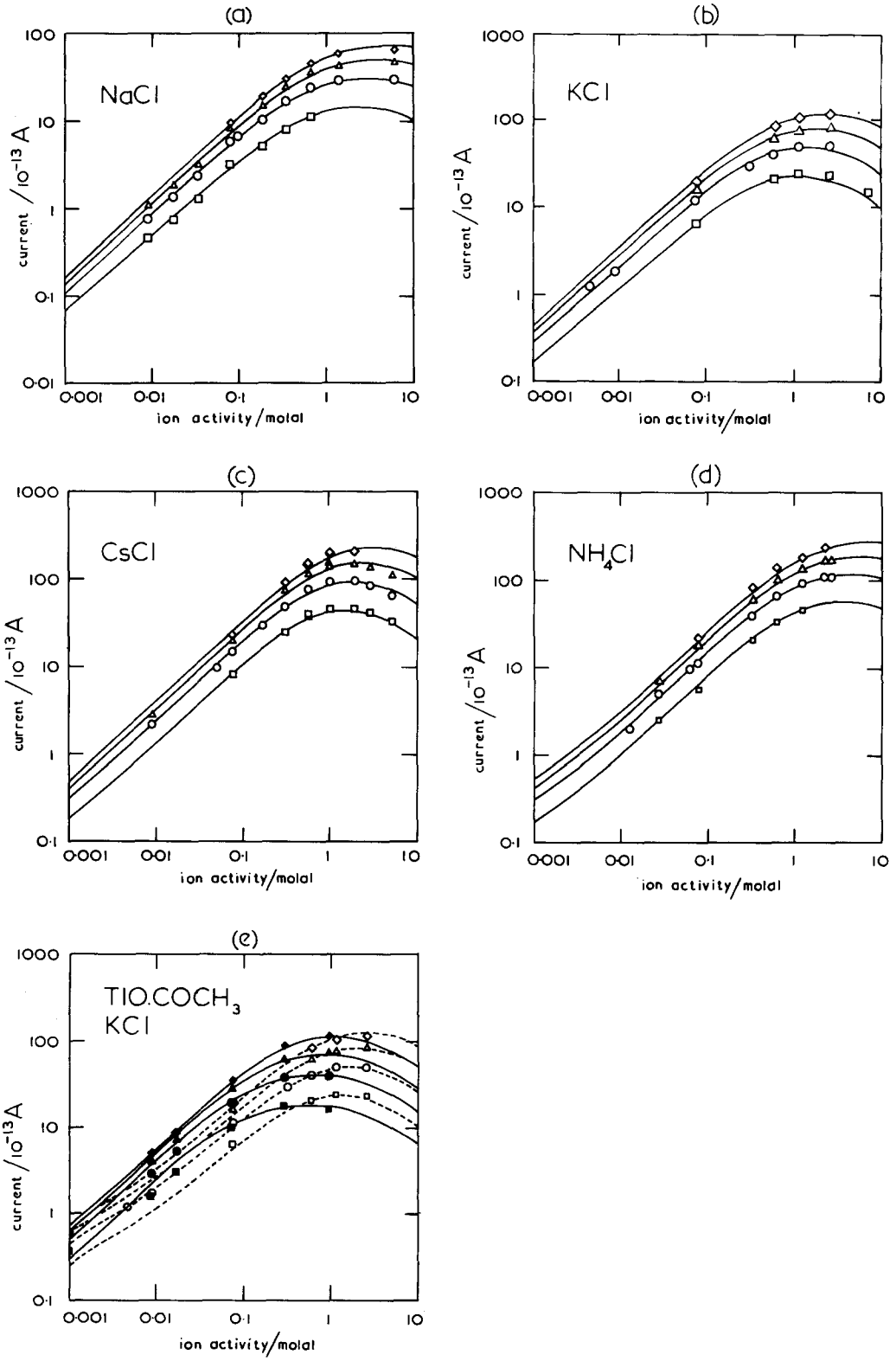

Fig. 2. Single-channel currents for NaCl, KCl, CsCl, NH_4Cl and $TlO \cdot COCH_3$ at four different membrane potentials (□, ■, 50 mV; ○, ●, 100 mV; △, ▲, 150 mV; ◇, ◆, 200 mV). For a—d the solid curves have been calculated from the rate constants of Table III. In e are shown currents for $TlO \cdot COCH_3$ (solid line, filled symbols) and KCl (dashed line, open symbols). The theoretical curves are based on constants from Table IV. Membranes were formed from glyceryl monooleate in hexadecane, T = 20—22° C.

measured. Their amplitudes are shown in Fig. 2 and listed in Appendix 3. Above 10 mM all the data are reproducible to within 10%. Below 10 mM the scatter is greater, possibly due to variable amounts of ionic impurities in the membrane lipid [24]. Only one negative charge in every 500 lipid molecules is needed to produce a surface potential of −10 mV, which is sufficient to increase the cation concentration near the membrane by a factor of 1.5; ionic impurities of this order of magnitude have been inferred to be present in glyceryl monooleate membranes [25].

Bi-ionic potentials

In bi-ionic potential measurements, the two compartments of the bilayer chamber were filled with different single-salt solutions of the same concentration and the potential which prevented current flow was measured. Bi-ionic potentials for various salt pairs across gramicidin-containing glyceryl monooleate/decane membranes are presented in Table II. The data points represent the mean of at least two separate experiments and were found to be very reproducible. Where comparable, they differ slightly from those of Myers and Haydon [6] due probably to improvements in the technique. In addition, bi-ionic potentials for gramicidin in glyceryl monooleate/hexadecane membranes were determined for (KCl, NaCl) at 1 and 100 mM. Within experimental error (0.2 mV), they came out to be the same as those for glyceryl monooleate/decane membranes. For all salt pairs, the permeability ratio is already concentration dependent in the lowest concentration ranges studied.

Whereas the single-channel conductances for Tl^+ are not very different from those for K^+, the bi-ionic potentials for Tl^+ compared to K^+ are large and those for Tl^+ compared to Na^+ are much greater than for K^+ compared to Na^+ [26].

When experimental data involving cation mixtures were examined with a view to determining values of rate constants [4], it was found that (particularly at high concentrations) the activities of the relevant mixed electrolytes were not accurately known. The resulting uncertainties were such that these data will not be used in rate-constant determinations.

TABLE II

EXPERIMENTAL BI-IONIC POTENTIALS

The corresponding permeability ratios are shown in Fig. 3. Values indicated by an asterisk were taken from Ref. 6. They were reproducible to within 1 mV, the other data within 0.5 mV. Large fluctuations (2 mV) occurred at 0.1 mM TlCl:KCl rendering this data point more inaccurate. The values for $TlNO_3$:KNO_3 may be less reliable because of a lesser purity of the $TlNO_3$ salt (see Materials and Methods).

Concentration (mM)	KCl:NaCl (mV)	CsCl:NaCl (mV)	NH_4Cl:NaCl (mV)	TlCl:NaCl (mV)	TlCl:KCl (mV)	$TlNO_3$:KNO_3 (mV)
0.1					25.7	
1	26.9	31.3	38 *	58.5		34.3
10	27.7	33.8	44 *	72.2	46.2	49.0
96						70.4
100	29.2	36.4	46 *			
286						76.5
1000	34.3	46.8	56 *			
3000	38 *	—	58 *			

Simplification of the model, and the curve fits: Rate constants for NaCl, KCl, CsCl and NH_4Cl

Even in the simplest, two-compartment description of a single-file pore, a large number of constants are required (see Appendices 1 and 2). Thus, to predict the current with a single species present, rate constants for transfer between the compartments (K), entry into either an empty pore (AA) or a pore occupied at the far end (DD), and exit from either a singly (B) or doubly occupied pore (E) must all be specified as functions of the potential *. Two rate constants for entry and exit are required, since two cations present simultaneously in the pore will repel each other. In preliminary attempts to fit the data for each salt using hand calculations, it was found that while a prohibition of double occupancy (i.e., $DD = 0$) was consistent with the available single-channel conductance data for NaCl, KCl and NH_4Cl, it was not so for CsCl. Furthermore, it was noted that even for the first three salts the constants determined on this basis failed to predict the observed [6] concentration-dependent bi-ionic potentials. Such variations are predicted by the present model, but only when the rate of entry of ions into occupied pores is significant [1,3,4,16]. It was also found that the current-voltage relationships could not be fitted assuming that K, the rate constant for crossing the central barrier, was the only constant to vary with potential.

From the preliminary observations it was apparent that it would be necessary to incorporate two compartments and all states of occupancy. However, this necessity does not imply a need to allow arbitrary variations of the constants with potential and the concentrations. It has therefore been assumed that the constants do not vary with concentration. The task of determining the constants is also greatly simplified if the possible potential dependence of the constants can be restricted by assuming plausible, simply adjustable functional forms. We have adopted those listed in Table VII (see Appendix 2) which allow the effect of a potential difference across the membrane to be partitioned into effects on the various constants, via the potential parameters C_1, C_2 and C_4 for each cation. The remaining constant, C_3, allows for variation in the assumed steepness and height of the barrier separating the compartments [2,27,28].

Even with these simplifications, separate fits for each salt to the single-channel conductance data do not determine the available constants. Additional information about the pore can be obtained by measuring zero-current potentials. In the general version of the two-compartment model when two species of ions are present, new rate constants (the parameters TT and Q, see Fig. 7 in Appendix 1) are required since the rates of entry into singly occupied pores and exit from doubly occupied pores can depend on the species of both ions in the pore. However, for cations with similar properties it is reasonable to expect that it will be the presence or absence of the second ion rather than its species which will be important, i.e., that approx. $DD = TT < AA$ and

* It is also possible that the so-called constants could vary with the ion concentrations in the aqueous phases. For instance, as the aqueous concentration of ions increases, the appearance of these phases to an ion within the pore would change from a dielectric to a good conductor which would change the force acting on that ion.

$E = Q > B$. This assumption greatly reduces the flexibility of the model but still fails to determine uniquely the values for the voltage parameters. Fits can, however, be obtained for all four salts based on the assumption that the potential dependence of each rate constant is independent of species. Separate curve fits had already produced results close to this approximation, and since it is unlikely to be critical, it has been made in all that follows.

The reader may now appreciate why no attempt has been made to include anion binding to the pore and thus increase the number of parameters that have to be determined. As discussed before, there is no evidence of an anion permeating the pore and therefore, to a first approximation, anions may be thought of as merely modulating cation entry and exit from the pore. The rate constants obtained here are therefore expected to change somewhat for salts made from different anions.

Using the initial guesses $DD = 0$ for Na^+, K^+ and NH_4^+, and $DD = AA$ for Cs^+, the assumptions discussed above, and error estimates based solely on experimental criteria (see Table VIII in Appendix 3), the least-squares minimization produced a fit (fit I [4,16]) which was unacceptable for the following reasons: (1) the rate constant for entry was larger if another cation was bound at the far end: (2) all the low-activity conductances were underestimated, and (3) the predicted current at 0.1 M increased more rapidly with potential than measured.

In order to remove these discrepancies, the low-conductance points were given a weight (see Appendix 3) much higher than experimental accuracy would allow. This is not an elegant procedure, but it has theoretical justification. The least-squares procedure used, i.e., the minimization of Eqn. 2, is sensitive only to the size and not to the sign of the differences between the predictions and the data points. If, as assumed in the procedure, the differences are due to random errors, roughly half should be of each sign. In the original fit the discrepancies were systematic, not random. These trends were obvious by inspection, but were not reflected in the function supplied for minimization. The final fit (see Figs. 2 and 3) resulting from the altered weights and the original fit as the initial guess, demonstrates the existence of a set of rate constants (Table III) such that the data can be predicted reasonably well without the systematic discrepancies noted above. The only alternative way to

TABLE III

VALUES OF RATE CONSTANTS AND VOLTAGE PARAMETERS AS OBTAINED FROM A SIMULTANEOUS SINGLE-CHANNEL CONDUCTANCE AND BI-IONIC DATA FIT

The data points used for the fit are listed in Appendix 3.

	Na^+	K^+	Cs^+	NH_4^+
AA [(mol/kg H_2O)$^{-1}$ · s^{-1}] ($X10^8$)	0.55	1.6	1.8	2.4
B (s^{-1}) ($X10^6$)	0.45	0.39	0.29	0.21
K (s^{-1}) ($X10^8$)	0.13	0.27	0.82	6.8
DD [(mol/kg H_2O)$^{-1}$ · s^{-1}] ($X10^8$)	0.53	1.4	1.6	1.2
E (s^{-1}) ($X10^8$)	2.6	2.1	1.6	0.63

$C_1 = 0.08$, $C_2 = 0.15$, $C_3 = 0.15$, $C_4 = 0.06$

force the fitting routine to notice these discrepancies would be to incorporate many more experimental points, particularly at low activities. Neher et al. [24] report single-channel conductance data at 50 mV membrane potential for a variety of salts, including more low-concentration points for the alkali-chloride salts than presented here. Incorporation of these would not change the nature of the final fit.

In principle, errors in the fitted rate constants could be estimated from the Jacobian matrix [22]. However, this would require a more realistic estimate for the weight of each data point than used here. Rather than paying too much attention to the absolute values of the rate constants, their relationships with respect to each other should be considered.

Rate constants for thallium

All attempts to include data for Tl^+ in the fits described above failed. There are at least two plausible explanations: (1) because of its low solubility, TlCl could not be used in many of the conductance measurements and anions other than Cl^- were normally present, and (2) Tl^+ is bound by sufficiently different parts of the pore that its interaction with any second ion present is significantly affected. The restrictive assumptions imposed above have thus been relaxed. As most of the bi-ionic data have been measured for the (Tl^+, K^+) system, curve fits have been run involving rate constants for just these two cations. The voltage parameters for Tl^+ were allowed to vary independently from those of

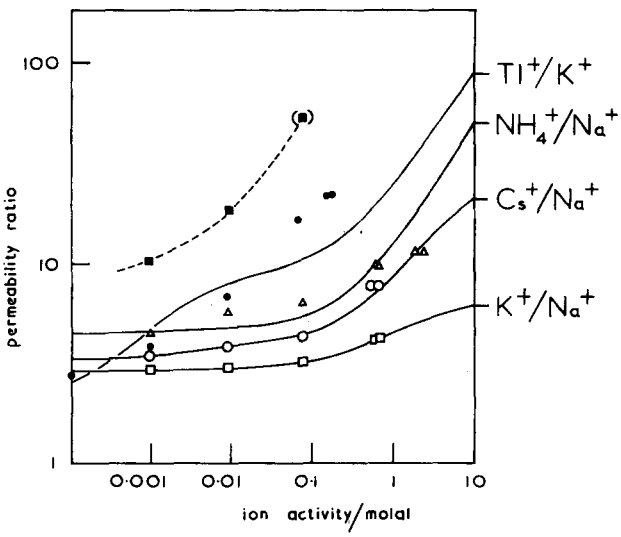

Fig. 3. Permeability ratios calculated from bi-ionic potentials and the Goldman-Hodgkin-Katz equation. The experimental points are: □, K^+/Na^+; ○, Cs^+/Na^+; △, NH_4^+/Na^+; ■, Tl^+/Na^+; ●, Tl^+/K^+. The 100 mM point for Tl^+/Na^+ has been obtained by multiplying the Tl^+/K^+ and K^+/Na^+ permeability at that concentration. Although in the experiment the concentration of the two salts on the opposite sites of the membrane were equal, their activities began to deviate significantly at high concentrations. To indicate this spread the permeabilities have been plotted twice with respect to the activity axis, corresponding to the two different salt activities. The solid curves have been calculated from the rate constants of Tables III and IV (T = 22° C). The dashed line was drawn by eye. Membranes were formed from glyceryl monooleate in decane, T = 20—22° C.

K^+ and the values of the K^+ rate constants to vary slightly from those in Table III. It is, however, still assumed that the rate constants of entry to singly occupied pores are independent of the species at the other end (i.e., $DD = TT$) and similarly for the rate constants for exit from doubly occupied pores ($Q = E$). Initial guesses for the rate constants of Tl^+ were obtained from the following. The ratio of B/AA was made to correspond to the activity at which a break appears in the linearity of the conductance-activity curve at low activities. The rate constant for entry of a second ion was estimated as $4GkT/e^2$ from the data at 0.1 M. AA is expected to be greater than DD without exceeding the diffusion limit. The experimental conductance-activity curve declines at high activities. The model predicts a decline proportional to $1/a$ when $D >> E$ and $D >> 2K$, from which a rough idea about the order of magnitude of K and E can be obtained.

Although it was possible to reproduce conductance and bi-ionic data very well on their own, when combined the agreement between experiment and prediction was only qualitative (see Figs. 2 and 3). Further relaxation of the assumptions to allow the rate constants to depend on the species of ion at the far end of the pore (i.e., $DD \neq TT$, etc.) would inevitably improve the fit dramatically [1,3], but this procedure introduces too many constants to be fitted.

Comparison of Model and Data

When judging the quality of fit it is important to take into account that all the predictions for NaCl, KCl, CsCl and NH_4Cl are based on a single set of rate constants as given in Table III, and similarly for the Tl^+-K^+ system shown in Table IV. No attempt has been made to improve appearances of figures by running fits that focus on any particular aspect of the data. The data presented here could be fitted much more closely by running curve fits in which all the rate constants available in a two-compartment pore are allowed to vary independently. This exercise would be meaningless as with the present set of data these rate constants could not be determined uniquely.

TABLE IV

VALUES OF RATE CONSTANTS AND VOLTAGE PARAMETERS AS OBTAINED FROM A SIMULTANEOUS SINGLE-CHANNEL CONDUCTANCE AND BI-IONIC DATA FIT

The data points used for the fit are listed in Appendix 3.

	Tl^+	K^+
AA [(mol/kg H_2O)$^{-1}$ · s^{-1}] ($X10^8$)	5.4	2.6
B (s^{-1}) ($X10^6$)	0.061	0.83
K (s^{-1}) ($X10^8$)	6.7	0.34
DD [(mol/kg H_2O)$^{-1}$ · s^{-1}] ($X10^8$)	3.7	1.1
E (s^{-1}) ($X10^8$)	0.15	1.3
C_1	0.13	0.17
C_2	0.13	0.000
C_3	0.23	0.15
C_4	0.002	0.07

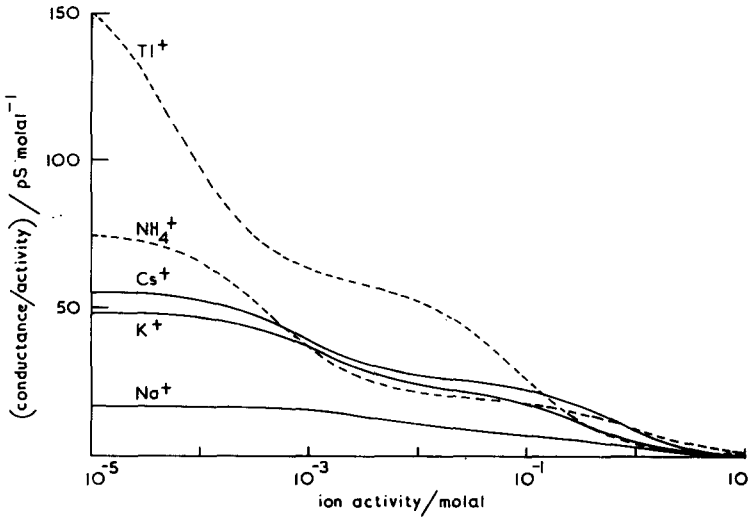

Fig. 4. Conductance divided by activity plotted versus activity for zero applied potential (see Eqn. 24 in Ref. 1) for the five cations, Na^+, K^+, Cs^+, NH_4^+ and Tl^+. Depending upon the cation, there are two more or less pronounced regions where the conductance increases linearly with activity, corresponding, respectively, to a pore which is most of the time either empty or significantly singly, but not doubly, occupied. Values of rate constants as in Table III for Na^+, K^+, Cs^+ and NH_4^+ and Table IV for Tl^+. $T = 22°C$.

Single-channel conductances and bi-ionic potentials

Fig. 2 shows calculated conductance curves and experimental data points. The log-log plots demonstrate very clearly the changing shape of the voltage dependence of the single-channel currents, which show a wider spread at higher activities. The explanation provided by the model for this change is that at low concentrations, filling the site from the aqueous compartment (which is relatively insensitive to voltage) constitutes the rate-limiting step, whereas translocation through the pore (which varies strongly with potential) becomes rate limiting at high concentrations [20,29]. The Tl^+ fit fails to predict currents very well at low activities. The conductances calculated at low potentials are shown in more detail in Fig. 4.

Fig. 3 compares experimental bi-ionic data with those theoretically calculated. A comparison of the permeabilities (see Fig. 3) for bi-ionic potential experiments shows that, as observed, the permeability ratios are predicted to rise at low concentrations. Bi-ionic potentials for Tl^+ are predicted to rise steeply all the time, except for a somewhat flatter region not experimentally observed.

Significance of the values of the rate constants

Finding a minimum for the sum of squares as given by Eqn. 2 is no guarantee that the correct set of rate constants has been found. The fitting routine does not register when the rate constants violate physical concepts, and therefore consistency with these constitutes an independent test on the validity of the rate constants obtained from a fit. The following observations deal with this point in more detail.

An ion entering an already singly occupied pore encounters an additional energy barrier, originating from electrostatic repulsion, which lowers the rate constant of entry and raises that of exit. The values of the rate constants in Tables III and IV are consistent in that the AA values are always larger than the DD values and the B values are considerably smaller than the E values. Also, as expected, the rate constants of exit are found to be more strongly affected than those of entry.

Besides the lower bound for AA set by DD, there also exists an upper bound derived from diffusion limitation. At very low concentrations and large applied potentials the ion flux through the pore is given by (see Ref. 1):

$$J = A' \tag{4}$$

The ionic diffusional flux can be roughly approximated as [30]:

$$J = 4D_{\mathrm{diff}}crL \tag{5}$$

where D_{diff} is the diffusion coefficient, c the concentration of the bulk solution, r is the radius of the mouth of the pore and L is Avogadro's constant. Dividing this flux by the activity and neglecting the effect of an electric field on diffusion, the diffusion limit for the rate constant AA is obtained and compared with the fit results in Table V. The rate constants of entry to an empty pore are consistent in that they do not exceed the diffusion limit. Table V suggests, however, that a diffusion barrier may exist for the more permeable ions. Andersen and Procopio [31] found that even entry of Na^+ was diffusion limited in diphytanoyl phosphatidylcholine bilayers.

Predictions

Occupancy

At an activity $a = B/(2AA)$, the probabilities of a pore being empty or singly occupied become equal. Similarly, at an activity $a = 2E/DD$, single and double occupancy of the pore are equally probable. Table VI shows for which activities the various cations begin to singly or doubly fill the pore. Significant single occupancy is predicted in the millimolar concentration range. The pore

TABLE V

COMPARISON OF THE DIFFUSION LIMIT FOR THE RATE CONSTANT AA WITH THE VALUES OBTAINED FROM THE CURVE FIT

D_{diff} is the diffusion coefficient at 25°C and infinite dilution. It has been calculated as the Nernst limiting value derived from the limiting mobilities of ions [32].

Salt	D_{diff} ($m^2 \cdot s^{-1}$) ($\times 10^{-9}$)	AA_{diff} [(mol/kg $H_2O)^{-1} \cdot s^{-1}$] ($\times 10^9$)	AA_{fit} [(mol/kg $H_2O)^{-1} \cdot s^{-1}$] ($\times 10^9$)
NaCl	1.61	0.78	0.055
KCl	1.99	0.96	0.16
CsCl	2.04	0.98	0.18
NH_4Cl	1.99	0.96	0.24
TlCl	2.01	0.97	0.54

TABLE VI

	Na^+	K^+	Cs^+	NH_4^+	Tl^+
$B/2AA$ (mol/kg H_2O) ($X10^{-3}$)	4.1	1.2	0.82	0.44	0.056
$2E/DD$ (mol/kg H_2O)	9.8	2.9	2.0	1.1	0.080

remains singly occupied for about three concentration decades before double occupancy becomes appreciable.

Unidirectional fluxes

Direct evidence for interactions in the gramicidin pore has come from unidirectional flux studies involving tracer cations. Schagina et al. [14] measured the exponent, n, appearing in the unidirectional flux ratios [1], and found for membranes made from bovine brain lipids that $n = 2.0$ for both 0.01 M and 0.1 M RbCl. Procopio and Andersen [15,33] used diphytanoyl phosphatidylcholine/n-decane bilayers and found no evidence for Na^+ interactions in the gramicidin channel, whereas 0.1 M and 1.0 M CsCl produced n values of approx. 1.4 and 1.6, respectively.

The predictions from the present fit are shown in Fig. 5 and are intermediate between the available experimental results. The present predictions are for channels in glyceryl monooleate membranes. It is known that gramicidin single-channel conductances in phospholipid membranes can be smaller by a factor of about 2 [34—39]. The reasons for this are not well understood and therefore quantitative agreement with either set of experiments cannot be expected.

Although Procopio and Andersen found no sign of Na^+ interaction in the gramicidin pore, streaming potential measurements by Levitt et al. [40] on

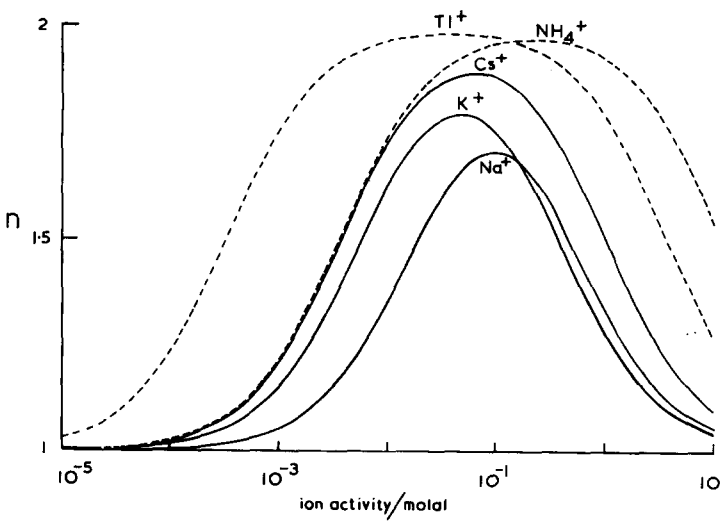

Fig. 5. The calculated flux-ratio exponent, n, versus activity (see Ref. 1, Eqn. 41). Values of rate constants as in Table III for Na^+, K^+, Cs^+ and NH_4^+ and Table IV for Tl^+. $T = 22°C$.

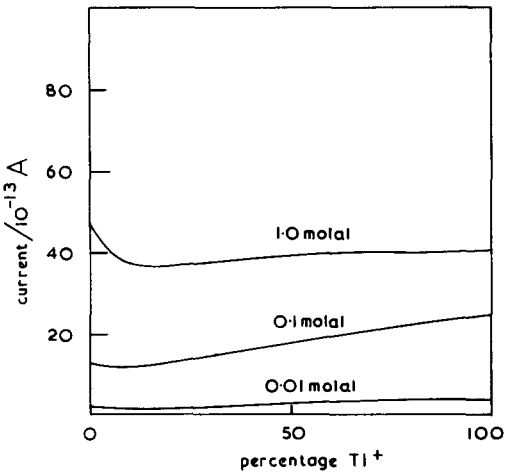

Fig. 6. The curves represent predicted single-channel currents (rate constants from Table IV) for symmetrical electrolyte mixtures of Tl^+ and K^+. The sum of the activities of Tl^+ and K^+ is kept constant for each curve. Percentage refers to activity. The membrane potential is 100 mV. $T = 22°C$.

glyceryl monooleate and Rosenberg and Finkelstein [41] on bacterial phosphatidylethanolamine could possibly suggest such interaction.

Blocking

In salt mixtures of Tl^+ and Na^+ at constant total concentration, Neher [42, 43] observed a particular type of blocking. When the single-channel conductances are plotted versus mole fraction of Tl^+, a minimum occurs near 98% Na^+, suggesting that in this mixture Tl^+ blocks Na^+.

It has been shown elsewhere [1,17] that the present model predicts a similar effect for Tl^+ and Na^+ with plausible values of the rate constants. Using the fitted constants (Table III), blocking of NaCl by KCl or CsCl is negligible. Adding NH_4Cl to NaCl at a total activity of 100 mM or 1 M with 50 mV applied potential, only a very shallow minimum in the conductance is predicted (less than 4%). In an experimental test, CsCl (1—50 mM) was added to 1 M NaCl. No minimum could be detected, only an increase in conductance. With Tl^+/K^+ the fitted constants (Table IV) predict a minimum in the conductance (see Fig. 6) at approximately the same activity as observed experimentally by Neher et al. (see Fig. 5 in Ref. 24) but is shallower than that found by these authors.

It should be noted that the data used to calculate the rate constants were obtained using solutions which contained various single salts. Nevertheless, for solutions containing salt mixtures, the model rightly predicts the presence or absence of block, and the mole fraction at which it occurs.

Discussion

The objective of this paper has been to find the simplest model which can account for our ion-flux data with gramicidin. Models which allow only one ion at a time to enter the pore are clearly excluded by the data. The concen-

tration dependence of the permeability ratio and the discrepancy between conductance and permeability ratios reported here and the tracer-flux ratios [14,15] have no other known explanation [1,16,17]. In addition, conduction by a two-ion process explains the shape of the conductance-activity relationships. It is thus appropriate to investigate the extent to which the two-compartment pore model with single-file restraint accounts for the existing flux data. However, while the physical model is simple, it already contains more adjustable parameters than can be determined from our data. Based on preliminary fits, the parameters were therefore divided into two classes according to whether or not they depended very strongly on ionic species. Only the parameters of the former class were allowed to take on different values for each species, while those of the latter class had to be the same for all ions. It was assumed that the cations bound to very similar sites and, consequently, the parameters describing the voltage dependence of the various rates were taken to be identical for each species. Furthermore, the rate constants for transitions involving a doubly occupied pore were assumed not to depend on the species of the ion which was not moving. Reasonable fits could be obtained, and it was observed that the rate constants change in a monotonic sequence from Na^+, K^+, Cs^+ to NH_4^+. However, NH_4^+ seems to interact more strongly with the second ion in the pore. Whereas for Na^+, K^+ and Cs^+ the rate constants AA and DD are almost equal, for NH_4^+ $AA \simeq 2DD$ is observed. This finding suggests a failure of the simplifying assumption that it is only the presence or absence of a second ion in the pore which matters and not its species.

In the case of Tl^+, these restrictive assumptions no longer allowed reasonable fits and they had to be partially relaxed. There are a number of observations which suggest that Tl^+ binds more strongly than the alkali cations to the gramicidin pore [4,26,42]. In view of this, it is understandable that Tl^+ displays at lower concentrations those features of the kinetic data which are due to ion interaction (steeply rising permeability ratios, a maximum and decline in the single-channel conductance, blocking in mixtures). NH_4^+ also showed a stronger binding than the alkali cations. The latter assume a noble gas configuration and should interact with the pore mainly electrostatically. NH_4^+ can form hydrogen bonds and because thallium has a substantially higher polarizability than the alkali cations [44], it is likely to show larger van der Waal's interactions with the walls of the pore. An increase in binding energy might thereby result, leading also to binding sites that differ from those of the alkali cations.

There are a number of possible extensions to this model which would enable data to be fitted more closely. Allowing the effect of ion interaction on rates to depend on the species of both ions has been discussed above. Another obvious change would be to add more binding sites [45,46]. In addition, there is the prospect of providing for the presence of water molecules in the pore explicity rather than implicity as at present. There is good and direct evidence [10,34, 40,41] that the gramicidin pore is normally filled with water. Thus, the entry of an ion which must displace water should be allowed to vary with the activity of the water. Such changes, if they occur, would show up at high salt concentrations when the water activity should be significantly reduced. Under the same conditions, the assumption of a linear relationship between the rate

constants of entrance to the pore (A, D, T) and the ionic activity may also be strained. Similarly, the present theory ignores the effect of changes in the ionic and water activity on the rate constant of transfer (K). Yet, the energy barrier connected with K is believed to be a consequence mainly of an image force [2], the magnitude of which will depend on values for the dielectric constants of the channel interior and the aqueous phases (see Appendix B of Ref. 2; and Ref. 47). The dielectric constant of the aqueous phase changes with increasing ionic activity [48]; how the dielectric constant of the channel interior (if at all a useful concept) varies with changes in contents is not known. Finally, the ion fluxes are known to be affected by a net osmotic movement of water through the channels. Clearly, here an extended theory is needed.

With so many possible changes to the model, it will be difficult to decide if a particular refinement improves the physical correspondence between the model pore and gramicidin. Better fits than those presented here are inevitable when the model is extended simply as a consequence of having increased the number of free parameters. Thus, a close fit is not in itself a guarantee that the model has been extended in the right direction. What will be needed is evidence that the nature of the observed effects requires the chosen type of modification.

Appendix 1

Flux equation

The model assumes the pore to have two sites, each of which can be empty or occupied by an ion of species a or b. Transitions between different states of

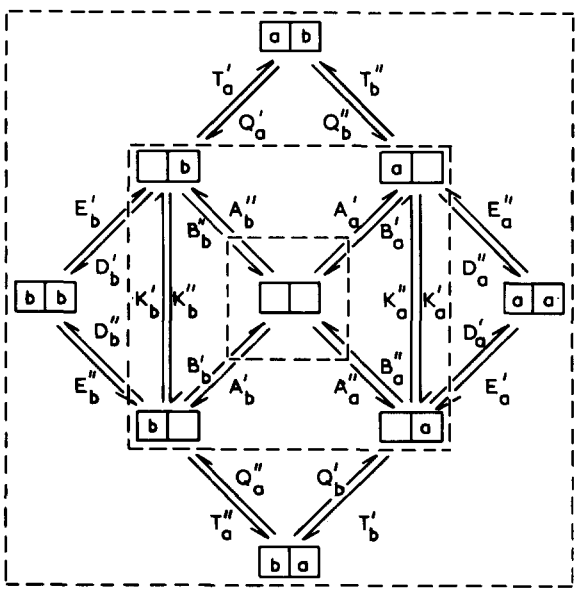

Fig. 7. Schematic representation of all the possible states of the two-compartment pore and the transitions between them, with their respective rate constants.

the pore occur at a rate which is equal to the product of the rate constant associated with this transition (A, B, K, D, T, E and Q) and the probability of the pore being in the initial state (P_{xy}). Rate constants, probabilities and auxiliary mathematical functions are denoted by a capital (occasionally two capitals) followed by two small letters representing their indices. Their meanings become more obvious from Fig. 7 (see Ref. 1 for further details). The activity dependence of the rate constants of entry have been assumed to be:

$$A_{xi} = AA_{xi} \cdot a_{xi}, \quad D_{xi} = DD_{xi} \cdot a_{xi}, \quad \text{and } T_{xi} = TT_{xi} \cdot a_{xi} \tag{1}$$

where AA_{xi}, DD_{xi} and TT_{xi} are now independent of both x and y ion concentrations. a_{xi} denotes the activity of species x in compartment i. TT_{xi} is independent of activity, but a function of the other ion species y in the channel.

The solution of the flux equation in terms of rate constants for the transition scheme in Fig. 7 can be calculated as follows [1]:

$$I = e[z_a(K'_a P_{ao} - K''_a P_{oa}) + z_b(K'_b P_{bo} - K''_b P_{ob})] \tag{2}$$

z_a and z_b are the respective valencies of ions a and b.

$$P_{oo} = D/DD \quad P_{ao} = N''_a/DD \quad P_{oa} = N'_a/DD \quad P_{bo} = N''_b/DD \quad P_{ob} = N'_b/DD \tag{3a–d}$$

$$N^i_x = -(A^j_x G^j_x + A^i_x F^i_x)(F^j_y F^i_y - G^j_y G^i_y) + G^j_x H^j_x (A^j_y F^j_y + A^i_y G^i_y)$$
$$+ F^i_x H^i_x (A^j_y G^j_y + A^i_y F^i_y) + A^i_x H^i_x H^j_y F^j_y - A^j_x H^i_x H^j_y G^j_y - A^i_y H^j_y H^j_x H^i_x \tag{4}$$

$$D = (F'_a F''_a - G'_a G''_a)(F'_b F''_b - G'_b G''_b) - F'_a F'_b H'_a H'_b - F''_a F''_b H''_a H''_b - G'_a G''_b H''_b H'_a$$
$$- G''_a G'_b H'_b H''_a + H'_a H'_b H''_a H''_b \tag{5}$$

$$DD = D + M'_a \cdot N'_b + M''_a \cdot N''_b + M'_b \cdot N'_a + M''_b \cdot N''_a \tag{6}$$

$$F^i_x = \left(K^i_x + \frac{E^i_x D^j_x}{E^i_x + E^j_x}\right) \quad M^i_x = \left(1 + \frac{T^i_x}{Q^i_x + Q^j_x} + \frac{D^i_y}{E^i_y + E^j_y}\right)$$

$$G^i_x = \left(\frac{D^i_x E^j_x}{E^i_x + E^j_x} + \frac{T^i_y Q^j_x}{Q^i_y + Q^j_x} + B^j_x + K^j_x\right) \quad H^i_x = \frac{T^i_x Q^j_y}{Q^j_y + Q^i_x} \tag{7a–d}$$

Appendix 2

Voltage dependence of the rate constants

The variations with potential of the various constants are restricted by the laws of microscopic reversibility as already discussed [1], but, in order to obtain a functional form for the rate constants, it is necessary to consider more restrictive assumptions for the potential dependence of the individual constants. Since the 'equilibrium constants', e.g., AA'/B', DD'/E', K'/K'', etc., are suitably taken to vary exponentially with the applied potential and in practice the precise form of the potential dependence chosen for each constant is found not to be critical, it will be assumed that all the rate constants except K vary exponentially. In preliminary fitting to the data for gramicidin, it was found that the voltage function for K' increased less steeply than a simple exponential, suggesting perhaps that K' and K'' represent diffusion over a wide energy barrier. A simple but arbitrary functional form

TABLE VII

THE ASSUMED POTENTIAL DEPENDENCE OF THE RATE CONSTANTS

$\phi = eV/(kT)$. V is the potential difference measured with respect to the side denoted by $''$; z_x, z_y are valencies. The quantities AA_x, B_x, K_x, DD_x, TT_x, E_x and Q_x are all independent of voltage, and will still be referred to as rate constants, whereas C_{x1}—C_{x4}, C_{y1}—C_{y4} and C_5—C_7 will be called voltage parameters.

$$A'_x = AA_x a'_x \exp(-z_x\phi C_{x1}) \qquad A''_x = AA_x a''_x \exp(z_x\phi C_{x1}) \quad (1)$$

$$B'_x = B_x \exp(z_x\phi C_{x2}) \qquad B''_x = B_x \exp(-z_x\phi C_{x2}) \quad (2)$$

$$K'_x = \frac{K_x \exp([C_{x1} + C_{x2} - 0.5]z_x\phi)}{\cosh(z_x\phi C_{x3})} \qquad K''_x = \frac{K_x \exp(-[C_{x1} + C_{x2} - 0.5]z_x\phi)}{\cosh(z_x\phi C_{x3})} \quad (3)$$

$$D'_x = DD_x a'_x \exp(-z_x\phi C_{x4}) \qquad D''_x = DD_x a''_x \exp(z_x\phi C_{x4}) \quad (4)$$

$$E'_x = E_x \exp([C_{x1} + C_{x2} - C_{x4}]z_x\phi) \qquad E''_x = E_x \exp(-[C_{x1} + C_{x2} - C_{x4}]z_x\phi) \quad (5)$$

Comparable expressions are used for the rate constants of ion species y.

$$T'_x = TT_x a'_x \exp(-z_x\phi C_5) \qquad T''_x = TT_x a''_x \exp(z_x\phi C_5) \quad (6)$$

$$Q'_x = Q_x \exp(z_x\phi C_6) \qquad Q''_x = Q_x \exp(-z_x\phi C_6) \quad (7)$$

$$T'_y = TT_y a'_y \exp(-z_y\phi C_7) \qquad T''_y = TT_y a''_y \exp(z_y\phi C_7) \quad (8)$$

$$Q'_y = Q_y \exp\{\phi[z_x(C_{x1} + C_{x2} - C_5 - C_6) + z_y(C_{y1} + C_{y2} - C_7)]\} \quad (9)$$

$$Q''_y = Q_y \exp\{-\phi[z_x(C_{x1} + C_{x2} - C_5 - C_6) + z_y(C_{y1} + C_{y2} - C_7)]\} \quad (10)$$

displaying this type of behaviour is an exponential divided by a cosh function containing another adjustable parameter. Finally, for application to gramicidin, it is possible to assume that the pore is symmetrical. The potential dependence of the rate constants corresponding to these assumptions is shown in Table VII.

Appendix 3

TABLE VIII

LISTING OF DATA WHICH HAVE BEEN USED FOR COMPUTER CURVE FITS (ALL ACTIVITIES ARE EXPRESSED IN MOLALITIES)

Single-channel conductance data. Column 1, salt activity; column 2, single-channel current in 0.1 pA; column 3, membrane potential in V; column 4, standard deviations in 0.1 pA; column 5, standard deviations for fit I (see Ref. 4) where these differ from the values of column 4. Bi-ionic potential data. Column 1, activity of first salt in left-hand compartment; column 2, activity of second salt (NaCl or KNO_3) in right-hand compartment; column 3, bi-ionic potential in V.

1	2	3	4	5	1	2	3	4	5
Single-channel conductance data									
NaCl									
0.0090	0.465	0.05	0.005	0.1	0.0175	0.743	0.05	0.05	0.1
0.0336	1.29	0.05	0.1	0.2	0.0790	3.19	0.05	0.2	0.35
0.188	5.10	0.05	0.5	1	0.3490	8.02	0.05	0.2	0.4
0.6700	11.28	0.05	0.4		0.009	0.75	0.10	0.0075	0.1
0.0175	1.35	0.10	0.1		0.0336	2.35	0.10	0.2	
0.0790	5.80	0.10	0.3	0.5	0.0970	6.70	0.10	1	
0.1088	10.2	0.10	1.0		0.3490	16.7	0.10	0.4	
0.6700	24	0.10	0.8	0.4	1.4000	28.5	0.10	1	
6.0400	29.5	0.10	2	1	0.0090	1.08	0.15	0.01	0.3
0.0175	1.796	0.15	0.3		0.0336	3.08	0.15	0.3	0.6
0.0790	8.03	0.15	0.5	1	0.1880	14.59	0.15	1.5	3
0.3490	24.55	0.15	0.6	1.2	0.6700	35.16	0.15	1.8	
1.4000	42.20	0.15	1.5	3	6.0400	46.60	0.15	3	
0.0790	9.43	0.20	0.6	1.9	0.1880	19.0	0.20	2	6
0.3490	30.06	0.20	0.8	1.6	0.6700	45.84	0.20	1.6	2.2
1.4000	58.2	0.20	2	6	6.0400	64.9	0.20	4	6

TABLE VIII (continued)

1	2	3	4	5	1	2	3	4	5
KCl									
0.077	6.52	0.05	0.3	1	0.620	21.17	0.05	0.5	
1.190	24.21	0.05	1.0		2.650	23.46	0.05	1.5	
0.00464	1.26	0.10	0.01266		0.009	1.80	0.10	0.018	0.2
0.077	12.00	0.10	0.5	1	0.325	33.00	0.10	0.5	
0.620	41.50	0.10	1		1.190	51.50	0.10	1	
2.650	51	0.10	2		0.077	16.76	0.15	0.75	2
0.620	64.33	0.15	1.5		1.190	77.77	0.15	3	
2.650	84.15	0.15	3		0.077	20.12	0.20	1	2.8
0.620	85.7	0.20	4.9		1.190	106.09	0.20	4	
2.650	117.56	0.20	5.06						
CsCl									
0.009	2.2	0.1	0.02	0.2	0.050	10	0.1	1	
0.076	15	0.1	1		0.170	30	0.1	1	
0.303	49	0.1	2		0.555	78	0.1	2	
0.993	94	0.1	2		1.890	97	0.1	2	
2.880	85	0.1	2		5.080	65	0.1	2	
0.555	19.3	0.025	1.1		0.993	23.1	0.025	1.2	
0.076	8.25	0.05	1.0		0.303	24.99	0.05	2.0	
0.555	38.22	0.05	2.0		0.555	39.0	0.05	2.2	
1.890	46.56	0.05	2.0		0.993	46.2	0.05	2.4	
2.880	42.5	0.05	10		5.080	33.15	0.05	2.0	
0.555	58.2	0.075	3.2		0.993	70.1	0.075	3.6	
0.555	97.7	0.125	5.4		0.993	118.3	0.125	6	
0.009	2.85	0.15	0.0285	0.4	0.076	20.25	0.15	1.8	
0.303	73.99	0.15	6.0		0.555	117	0.15	6.0	
0.555	116.6	0.15	6.5		0.993	148.5	0.15	6.0	
0.993	142.7	0.15	7.3		1.890	150.4	0.15	6.0	
2.880	140.3	0.15	6.0		5.080	111.2	0.15	6.0	
0.555	136.5	0.175	7.6		0.993	169.4	0.175	8.6	
0.076	23.03	0.2	3.0		0.303	93.59	0.2	8.0	
0.555	156	0.2	8.0		0.555	151.7	0.2	8.6	
0.993	202.1	0.2	10.4		0.993	195.2	0.2	9.9	
1.890	208.5	0.2	8.0		0.993	252.6	0.25	12.6	
0.555	214.5	0.3	12.4		0.993	301.3	0.3	15.0	
0.993	355.7	0.35	17.7						
NH_4Cl									
0.0127	2.0	0.10	0.2		0.0270	5.1	0.10	0.5	
0.0625	9.9	0.10	0.2		0.0770	11.5	0.10	0.5	
0.3300	40.0	0.10	1		0.6300	67.0	0.10	1	
1.2300	93.0	0.10	2.5		2.2400	113	0.10	3.0	
2.6500	110	0.10	2.5		0.0270	2.55	0.05	0.5	
0.0770	5.75	0.05	0.8		0.3300	21.2	0.05	1	
0.6300	33.5	0.05	1		1.2300	45.57	0.05	2.5	
0.0270	7.14	0.15	1.5		0.0770	18.29	0.15	1.8	
0.3300	61.60	0.15	3.1		0.6300	102.5	0.15	3.5	
1.2300	137.6	0.15	7.5		2.2400	172.9	0.15	9.0	
2.6500	170.5	0.15	7.5		0.0770	21.85	0.20	2.0	
0.3300	82.00	0.20	4.0		0.6300	139.0	0.20	8.0	
1.2300	184.1	0.20	10.0		2.2400	234.5	0.20	11.5	
TlCl (data point at 1 mM), $TlO \cdot COCH_3$ (rest):									
0.000962	0.385	0.05	0.0077		0.00898	1.685	0.05	0.0843	
0.01730	3.075	0.05	0.3075		0.0745	10.335	0.05	0.5167	
0.3020	18.04	0.05	0.902		0.9810	16.63	0.05	0.831	
0.000962	0.60	0.1	0.012		0.00898	2.99	0.1	0.1495	
0.01730	5.39	0.1	0.539		0.0745	19.90	0.1	0.95	
0.3020	39.06	0.1	1.953		0.9810	39.95	0.1	1.997	
0.00898	4.08	0.15	0.204		0.01730	7.53	0.15	0.753	
0.0745	28.56	0.15	1.428		0.3020	63.44	0.15	3.172	
0.9810	74.45	0.15	3.722		0.00898	5.12	0.2	0.256	
0.01730	9.06	0.2	0.906		0.0745	36.02	0.2	1.801	
0.3020	90.4	0.2	4.52		0.9810	116.78	0.2	5.839	

TABLE VIII (continued)

1	2	3
Bi-ionic potential data		
KCl/NaCl		
0.000965	0.000965	0.0269
0.00901	0.00902	0.02772
0.0773	0.0781	0.02919
0.621	0.670	0.03432
CsCl/NaCl		
0.000965	0.000965	0.03130
0.00899	0.00902	0.03376
0.0760	0.0781	0.03637
0.565	0.670	0.04675
NH_4Cl/NaCl		
0.000965	0.000965	0.038
0.00901	0.00902	0.044
0.0774	0.0781	0.046
0.625	0.670	0.056
1.902	2.321	0.058
$TlNO_3/KNO_3$		
0.00009882	0.00009885	0.0257
0.000962	0.0009666	0.0343
0.00890	0.00899	0.049
0.06719	0.07073	0.07035
0.1584	0.1777	0.0765

References

1 Urban, B.W. and Hladky, S.B. (1979) Biochim. Biophys. Acta 554, 410—429
2 Haydon, D.A. and Hladky, S.B. (1972) Q. Rev. Biophys. 5, 187—282
3 Hladky, S.B. (1972) The Mechanism of Ion Conduction in Thin Lipid Membranes Containing Gramicidin A, Ph. D. dissertation, University of Cambridge
4 Urban, B.W. (1978) The Kinetics of Ion Movements in the Gramicidin Channel, Ph. D. dissertation, University of Cambridge
5 Bamberg, E. and Läuger, P. (1977) J. Membrane Biol. 35, 351—375
6 Myers, V.B. and Haydon, D.A. (1972) Biochim. Biophys. Acta 274, 313—322
7 Pressman, B.C. (1963) in Energy-linked Functions of Mitochondria Biochemistry (Chance, B., ed), pp 181—216, Academic Press, New York
8 Chappell, J.B. and Crofts, A.R. (1965) Biochem. J. 95, 393—402
9 Muller, P. and Rudin, D.O. (1967) Biochem. Biophys. Res. Commun. 26, 398—404
10 Hladky, S.B. and Haydon, D.A. (1972) Biochim. Biophys. Acta 274, 294—312
11 Urry, D.W., Goodall, M.C., Glickson, J.D. and Myers, D.F. (1971) Proc. Natl. Acad. Sci. U.S.A. 68, 1907—1911
12 Bamberg, E., Apell, H.J. and Alpes, H. (1977) Proc. Natl. Acad. Sci. U.S.A. 74, 2402—2406
13 Morrow, J.S., Veatch, W.R. and Stryer, L. (1978) J. Mol. Biol. 132, 733—738
14 Schagina, L.V., Grinfeldt, A.E. and Lev, A.A. (1978) Nature 273, 243—245
15 Procopio, J. and Andersen, O.S. (1979) Biophys. J. 25, 8a
16 Urban, B.W., Hladky, S.B. and Haydon, D.A. (1978) Fed. Proc. 37, 2628—2632
17 Hladky, S.B., Urban, B.W. and Haydon, D.A. (1979) in Membrane Transport Processes (Stevens, C. and Tsien, R.W., eds.), pp. 89—103, Raven Press, New York
18 Bamberg, E., Noda, K., Gross, E. and Läuger, P. (1976) Biochim. Biophys. Acta 419, 223—228
19 Fettiplace, R., Gordon, L.G.M., Hladky, S.B., Requena, J., Zingsheim, H.P. and Haydon, D.A. (1975) in Methods in Membrane Biology (Korn, E.D., ed.), Vol. 4, pp. 1—75, Plenum Press, New York
20 Hladky, S.B. and Haydon, D.A. (1972) in Symposium of Molecular Mechanisms of Antibiotic Action on Protein Biosynthesis and Membranes (Munoz, E., Garcia-Ferrandiz, F. and Vazquez, D. eds.), pp. 738—753, Elsevier, Amsterdam
21 NAG Fortran Library Manual, Mark 5 (FLM5) (1977) EO4FBF-NAGFLIB : 1308/329 : Mk5 : Nov. 75. Numerical Algorithms Group; 7 Banbury Road, Oxford OX2 6NN

22 Becington, P.R. (1969) Data Reduction and Error Analysis for the Physical Sciences, McGraw-Hill, New York
23 Glasstone, S. and Lewis, D. (1960) Elements of Physical Chemistry, 2nd edn., Macmillan, London
24 Neher, E., Sandblom, J. and Eisenman, G. (1978) J. Membrane Biol. 40, 97—116
25 White, S.H. (1973) Biochim. Biophys. Acta 323, 343—350
26 Eisenman, G., Sandblom, J. and Neher, E. (1976) in 9th Jerusalem Symposium on Metal-ligand Interaction in Organic and Biochemistry (Pullman, B. and Goldblum, N.D., eds.), pp. 1—36, Reidel, Dordrecht, The Netherlands
27 Andersen, O.S. (1978) in Membrane Transport in Biology, I. Concepts and Models. (Giebisch, G., Tosteson, D.C. and Ussing, H.H., eds.), pp. 369—446, Springer-Verlag, Berlin
28 Hladky, S.B. (1979) in Current Topics in Membranes and Transport (Bronner, F. and Kleinzeller, A., eds.), Vol. 12, Academic Press, New York
29 Haegglund, J., Enos, B. and Eisenman, G. (1979) Brain Res. Bull. 4, 154—158
30 Carslaw, H.S. and Jaeger, J.C. (1959) Conduction of Heat in Solids, Oxford University Press
31 Andersen, O.S. and Procopio, J. (1978) Biophys. J. 21, 26a
32 Robinson, P.A. and Stokes, R.H. (1965) Electrolytes, Butterworth, London
33 Andersen, O.S. and Procopio, J. (1980) Acta Physiol. Scand. Suppl., in the press
34 Finkelstein, A. (1974) in Drrugs and Transport Processes (Callingham, B.A., ed.), pp. 241—250, Macmillan, London
35 Zingsheim, H.P. and Neher, E. (1974) Biophys. Chem. 2, 197—207
36 Kolb, H.A., Läuger, P. and Bamberg, E. (1975) J. Membrane Biol. 20, 133—154
37 Bamberg, E. and Benz, R. (1976) Biochim. Biophys. Acta 426, 570—580
38 Kolb, H.A. and Bamberg, E. (1977) Biochim. Biophys. Acta 464, 127—141
39 Neher, E. and Eibl, H. (1977) Biochim. Biophys. Acta 464, 37—44
40 Levitt, D.G., Elias, S.R. and Hautman, J.M. (1978) Biochim. Biophys. Acta 512, 436—451
41 Rosenberg, P.A. and Finkelstein, A. (1978) J. Gen. Physiol. 72, 327—340
42 Neher, E. (1975) Biochim. Biophys. Acta 401, 540—544
43 Neher, E. (1977) Erratum, Biochim. Biophys. Acta 469, 359
44 Moelwyn-Hughes, E.A. (1961) Physical Chemistry, 2nd revised ed., p. 400, Pergamon Press, Oxford
45 Levitt, D.G. (1978) Biophys. J. 22, 221—248
46 Eisenman, G., Sandblom, J. and Enos, B. (1978) Biophys. J. 21, 26a
47 Neumcke, B. and Läuger, P. (1969) Biophys. J. 9, 1160—1170
48 Hasted, J.B. (1973) in Studies in Chemical Physics, pp. 136—137, Chapman and Hall, London